Decreasing Indian summer monsoon in northern Indian sub-continent during the last 180 years: evidence from five tree cellulose oxygen isotope chronologies

Chenxi Xu[1], Masaki Sano[2,3], A. P. Dimri[4], Rengaswamy Ramesh[5,6], Takeshi Nakatsuka[2], Feng Shi[1], Zhengtang Guo[1,7,8]

1. Key Laboratory of Cenozoic Geology and Environment, Institute of Geology and Geophysics, Chinese Academy of Sciences, Beijing 100029, China
2. Research Institute for Humanity and Nature, 457-4 Motoyama, Kamigamo, Kita-ku, Kyoto, Japan
3. Faculty of Human Sciences, Waseda University, 2-579-15 Mikajima, Tokorozawa 359-1192, Japan
4. School of Environmental Sciences, Jawaharlal Nehru University, New Delhi, India
5. Geoscience Division, Physical Research Laboratory, Navrangpura, Ahmedabad 380009, India
6. School of Earth and Planetary Sciences, National Institute of Science Education and Research, Odisha 752050, India
7. CAS Center for Excellence in Tibetan Plateau Earth Sciences, Beijing 100101, China
8. University of Chinese Academy of Sciences, Beijing, China

Correspondence to: Masaki Sano, (msano@aoni.waseda.jp)

Abstract. We have constructed a regional tree ring cellulose oxygen isotope ($\delta^{18}O$) record for the northern Indian sub-continent based on two new records from north India and central Nepal and three published records from Northwest India, western Nepal and Bhutan. The record spans the common interval from 1743-2008 CE. Correlation analysis reveals that the record is significantly and negatively correlated with the three regional climatic indices: All India Rainfall (r = -0.5, p <0.001, n =138), Indian monsoon index (r = -0.45, p <0.001, n =51) and the intensity of monsoonal circulation (r = -0.42, p <0.001, n =51). The close relationship between tree ring cellulose $\delta^{18}O$ and the Indian summer monsoon (ISM) can be explained by oxygen isotope fractionation mechanisms. Our results indicate that the regional tree ring cellulose $\delta^{18}O$ record is suitable for reconstructing high-resolution changes in the ISM. The record exhibits significant inter-annual and centennial variations. Inter-annual changes are closely related to the El Niño-Southern Oscillation (ENSO), which indicates that the ISM was affected by ENSO in the past. However, the ISM-ENSO relationship was not consistent over time. Centennial changes in the regional tree ring $\delta^{18}O$ record indicate a trend of weakened ISM intensity since 1820. Decreasing ISM activity is also observed in various high-resolution ISM records from southwest China and Southeast Asia, and may be the result of reduced land-ocean thermal contrasts since 1820 CE.

1 Introduction

The Indian summer monsoon (ISM) delivers a large amount of summer precipitation to the Indian continent, and thus has a major influence on economic activity and society in this densely-populated region (Webster et al., 1998). Current research on the ISM is mainly concerned with the study of inter-annual and inter-decadal variations, using meteorological data and climate models. El Niño-Southern Oscillation (ENSO) has great influences on ISM at inter-annual time scales, and El Niño events (Warm phase of ENSO) usually produced ISM failure (Kumar et al., 1999; Kumar et al., 2006; Webster et al., 1998). North Atlantic Sea surface temperature (SST) affected ISM by modulating tropospheric temperature over Eurasia (Goswami et al., 2006; Kripalani et al., 2007). Climate model experiments indicate that there is a significant increase in mean ISM precipitation of 8% under the doubling atmospheric carbon dioxide concentration scenario (Kripalani et al., 2007) and human-influenced aerosol emissions mainly resulted in observed precipitation decrease during the second half of the 20th century (Bollasina and Ramaswamy, 2011). A good understanding of mechanisms driving ISM change on different time scales could help to predict possible changes of ISM in the future. However, the observed meteorological records are too short to assess centennial changes in ISM. Therefore, long-term proxy records of ISM are needed.

The abundance of *Globigerina bulloides* in marine sediment cores from the Arabian Sea indicated a trend of increasing ISM strength during the last 400 years (Anderson et al., 2002). However, oxygen isotopes in tree-rings and ice cores from the Tibetan Plateau revealed a weakening trend ISM since 1840 or 1860 (Duan et al., 2004; Grießinger et al., 2016; Liu et al., 2014; Wernicke et al., 2015). Monsoon precipitation in northwestern India showed a significant decreasing trend during the period of 1866-2006 (Bhutiyani et al., 2010). In addition, a stalagmite oxygen isotope record from northern India indicated that the ISM experienced a 70-year pattern of variation over the last 200 years, with no clear trend (Sinha et al., 2015). Since there are spatial differences in the patterns of climate change in monsoonal areas (Sinha et al., 2011), geological records with

a wide distribution are needed. In addition, the climate proxies should be closely related to the ISM and the records need to be well-replicated and accurately dated.

Available tree ring records are widely distributed in the Indian monsoon region (Yadav et al., 2011). The climate of the southern Himalayas is dominated by changes in the Indian summer monsoon, and therefore the region is well suited to the study of Indian monsoon variations. The oxygen isotopic composition ($\delta^{18}O$) of tree rings is mainly controlled by the $\delta^{18}O$ of precipitation and by relative humidity (Ramesh et al., 1985; Roden et al., 2000), and both are affected by the Indian summer monsoon (Vuille et al., 2005). Compared with tree ring width data, tree ring $\delta^{18}O$ records are more suited to retrieving low-frequency climate signals, and therefore they have the ability to record the Indian summer monsoon (Gagen et al., 2011; Sano et al., 2012; Sano et al., 2013). In addition, tree ring $\delta^{18}O$ is considered as a promising proxy for next phase of Past Global Changes (PAGES) 2k network not only for hydroclimate reconstruction in Asia but also for data-model comparison to understand the mechanisms of climate variability at decadal to centennial timescales.

PAGES launched 2k network that produced regional and global temperature and precipitation syntheses based on multi-proxy and multi-record to obtain a better understanding of regional and global climate change. The ISM affected the large area of Indian continent, and a local record may not be fully representative of changes in the ISM. Therefore, we produced regional syntheses based on several tree ring $\delta^{18}O$ records from the ISM region. Two new records from northern India and central Nepal were obtained in this study, and were combined with three previously published records from northwest India, western Nepal and Bhutan (Sano et al., 2012; Sano et al., 2013; Sano et al., In press). The data were integrated in order to produce a regional tree ring $\delta^{18}O$ record which was used to reconstruct the history of the ISM during the last several hundred years, and to investigate its possible driving mechanisms on various time scales.

2 **Materials and methods**

2.1 Sampling sites

Five tree ring cellulose $\delta^{18}O$ records were selected to construct a regional climate signal for the southern Himalaya (Figure 1). Three records (Manali, in northwest India; Humla, in west Nepal; and Wache, in Bhutan) were published previously (Sano et al., 2012; Sano et al., 2013; Sano et al., In press). Two tree ring cellulose $\delta^{18}O$ chronologies were constructed in this study. Core samples for *Cedrus deodara* near Jageshwar (29˚38'N, 79˚51'E, 3849 m a.s.l., JG) and *Abies spectabilis* near Ganesh (28°10'N, 85°11'E, 3550 m a.s.l.) were collected in 2009 and 2001, respectively. Information about each sampling site is shown in Table 1. In general, two core samples for each tree were collected at breast height using a 5-mm diameter increment corer. The cores were air dried at room temperature for 2-3 days and the surfaces were then smoothed with sand paper to render the ring boundaries clearly visible. The ring widths of the samples were measured at a resolution of 0.01mm using a binocular microscope with a linear stage interfaced with a computer (Velmex™, Acu-Rite). Cross dating was performed in the laboratory by matching variations in ring width from all cores to determine the calendar year of each ring. Quality control was conducted using the COFECHA computer program (Holmes, 1983).

2.2 Cellulose extraction and isotope measurements

Four trees near Ganesh and three trees near Jageshwar, all with relatively wide rings, were selected for oxygen isotope analysis (Figures 2 & 3). The modified plate method (Xu et al., 2011; Xu et al., 2013b, Kagawa et al., 2015), based on the chemical treatment procedure of the Jayme-Wise method (Green, 1963; Loader et al., 1997), was used to extract α-cellulose. The plate method of extracting α-cellulose directly from the wood plate rather than from individual rings can reduce the α-cellulose extraction time (Xu et al., 2011). In addition, the modified plate method can reduce the amount of sample material lost during cellulose extraction, enabling sufficient material to be obtained to enable narrow rings to be measured by isotope ratio mass

spectrometer (Xu et al., 2013b). There is no statistically significant difference between tree ring $\delta^{18}O$ values obtained by the plate and conventional methods (Kagawa et al., 2015; Xu et al., 2013b).

Cellulose samples (sample weight, 120-260 μg) were wrapped in silver foil, and tree ring cellulose oxygen isotope ratios ($^{18}O/^{16}O$) were measured using an isotope ratio mass spectrometer (Delta V Advantage, Thermo Scientific) interfaced with a pyrolysis-type high-temperature conversion elemental analyzer (TC/EA, Thermo Scientific) at the Research Institute for Humanity and Nature, Japan. Cellulose $\delta^{18}O$ values were calculated by comparison with Merck cellulose (laboratory working standard), which was inserted after every eight tree samples during the measurements. Oxygen isotope results are presented using the δ notation as the per mil (‰) deviation from Vienna Standard Mean Ocean Water (VSMOW): $\delta^{18}O = [(R_{sample}/R_{standard}) - 1] \times 1000$, where R_{sample} and $R_{standard}$ are the $^{18}O/^{16}O$ ratios of the sample and standard, respectively. The analytical uncertainty for repeated measurements of Merck cellulose was approximately ±0.15‰.

2.3 Climate analyses and Statistical Analysis

In the northern Indian subcontinent, the monsoon season is from June to September. The summer monsoon season supplies 78% and 83% of the annual precipitation for Kathmandu and New Delhi, respectively. The Indian monsoon index (IMI) (Wang et al., 2001, http://apdrc.soest.hawaii.edu/projects/monsoon/definition.html), the intensity of monsoon circulation (Webster and Yang, 1992) and All India Rainfall (AIR, obtained from the Indian Institute of Tropical Meteorology, Pune, India, Mooley et al., 2016) were selected as proxies for the Indian summer monsoon in order to investigate the relationship between tree ring cellulose $\delta^{18}O$ variations and the monsoon. In addition, we used the Royal Netherlands Meteorological Institute Climate Explorer (http://www.knmi.nl/) to determine spatial correlations between tree-ring cellulose $\delta^{18}O$, precipitation (GPCC V7) and sea-surface temperature (SST) values obtained from the National Climatic Data Center v4 data set. Temperature reconstructions for the Indian Ocean (Tierney et al., 2015) and the Tibetan Plateau (Cook et al., 2013; Shi et al., 2015; Wang

et al., 2015), spanning the last 400 years, were used to obtain a record of the history of land-ocean thermal contrast. The software "kSpectra Toolkit" was employed to calculate power spectrum of the regional tree ring oxygen isotope chronology. The 95% (±1.96σ) confidence limits for each chronology and the regional chronology were calculated to show the uncertainty of each chronology and the regional chronology, respectively (except for the tree-ring chronology from Hulma, western Nepal, because the chronology was produced by pooling method, and therefore the uncertainty of this chronology was not able to show).

3 Results and discussion

3.1 Tree ring $\delta^{18}O$ variations in the southern Himalaya and a regional tree ring $\delta^{18}O$ record

The oxygen isotopes of four individuals of *Abies spectabilis* in Ganesh (GE, central Nepal) and three individuals of *Cedrus deodara* in Jageshwar (JG, northern India) were measured for the interval from 1801-2000 CE and 1643-2008 CE, respectively. Individual tree ring $\delta^{18}O$ time series from four cores from central Nepal are shown in Figure 2a. The mean values (standard deviations) of the $\delta^{18}O$ time series from 224c, 233b, 235b, and 226a are 23.09‰ (1.22‰), 22.66‰ (1.27‰), 21.87‰ (1.12‰), and 22.94‰ (1.42‰), respectively, from 1901-2000 CE. The inter-tree differences in $\delta^{18}O$ values are small. The $\delta^{18}O$ values of the four cores exhibit peaks in 1813. The mean inter-series correlations (Rbar) among the cores range from 0.56-0.78 (Figure 2c), based on a 50-year window over the interval from 1801-2000 CE.

Three tree ring $\delta^{18}O$ time series from northern India (JG) are shown in Figure 3a. The mean values (standard deviations) of the $\delta^{18}O$ time series from 101c, 102c, and 103a are 30.11‰ (1.49‰), 29.7‰ (1.62‰) and 29.47‰ (1.53‰), respectively, over the interval from 1694-2008 CE. Three tree ring $\delta^{18}O$ time series in JG exhibit a consistent pattern of variations. The mean inter-series correlations (Rbar) among the cores range from 0.61-0.78 (Figure 3c), based on a 50-year window over the interval from 1641-2008 CE.

In northern Indian sub-continent, three long-term tree ring $\delta^{18}O$ chronologies from northwest India, eastern Nepal and Bhutan have been built up in previous studies (Sano et al., 2012; Sano et al., 2013; Sano et al., In press, Figure 4). Two tree ring $\delta^{18}O$ chronologies in this study and three tree ring $\delta^{18}O$ chronologies in previous studies originate in monsoonal area (Figure 1). Three tree ring $\delta^{18}O$ chronologies in northwest India, eastern Nepal and Bhutan were controlled by monsoon season rainfall or PDSI (Sano et al., 2012; Sano et al., 2013; Sano et al., In press, Table 1), and the two new tree ring $\delta^{18}O$ records obtained in the present study (JG and Ganesh) are negatively correlated with June-September PDSI in northern India (Table 1). In addition, the five tree ring $\delta^{18}O$ records for the Himalaya region are significantly correlated with one another at inter-annual time scale during the common period, and in most cases 31-year running averages of five tree ring $\delta^{18}O$ chronologies show significant correlations at multi-decadal time scale (Table 2). These results indicate that five tree ring $\delta^{18}O$ records reflect a common controlling factor that may be related to regional climate. Therefore, we combined two tree ring $\delta^{18}O$ records in this study with three previously published tree ring $\delta^{18}O$ chronologies to construct a regional tree ring $\delta^{18}O$ record. The five $\delta^{18}O$ records were individually normalized over the interval from 1801-2000 CE, and then averaged to produce a regional Himalayan $\delta^{18}O$ record (H5 $\delta^{18}O$ record) for the entire interval (Figure 4f). Only one chronology (JG) spans an interval prior to 1742 CE, and therefore we focus on the interval from 1743-2008 CE in this study.

3.2 Climatic signals in the regional tree ring $\delta^{18}O$ chronology

We assessed the potential of the H5 $\delta^{18}O$ record as an indicator of past monsoon changes by correlating it with All India Rainfall (AIR), the Indian Monsoon Index (IMI) and the intensity of monsoon circulation. The results revealed a significant negative correlation with AIR (r = -0.5, p <0.001, n =138), IMI (r = -0.45, p <0.001, n =51) and the intensity of the monsoon circulation (r = -0.42, p <0.001, n =51) (Figure 5). In addition, the results of spatial correlation analyses reveal that the H5

$\delta^{18}O$ record is negatively correlated with gridded June-September precipitation in northwest and northern India and Nepal (Figure 6). These findings indicate that the H5 $\delta^{18}O$ record is capable of reflecting ISM changes from a statistical perspective.

Tree ring $\delta^{18}O$ has a close relationship with the ISM based on tree ring cellulose oxygen isotope fractionation model. Precipitation $\delta^{18}O$ and relative humidity are the two main factors controlling tree ring $\delta^{18}O$ (Roden et al., 2000), and both are related to ISM changes in the monsoonal area. There is a negative correlation between the ISM and precipitation $\delta^{18}O$ in the monsoonal area (Vuille et al., 2005; Yang et al., 2016). Asian summer monsoon affects the $\delta^{18}O$ of precipitation through the amount effect (Cai and Tian, 2016; Lekshmy et al., 2015; Dansgaard, 1964). A stronger summer monsoon usually brings more summer rainfall to the southern Himalaya. The removal of the heavier isotopes during the condensation process results in the oxygen isotopic depletion of the water vapor. The greater the total amount of precipitation, and the stronger the convection, the more the oxygen isotopic composition of the rainwater is affected by depletion (Lekshmy et al., 2014; Vuille et al., 2003), and this signal is reflected in tree ring $\delta^{18}O$ values. In addition, monsoon-related factors (e.g. upstream rainout process) other than the ‘‘amount effect’’ may affect precipitation $\delta^{18}O$ significantly (Vuille et al., 2005). On the other hand, a stronger ISM leads to higher relative humidity, and a lower re-evaporation rate for rainfall or a reduced evaporation of leaf water in trees, resulting in less enriched tree ring $\delta^{18}O$ values (Risi et al., 2008; Roden et al., 2000).

3.3 Interannual variability of the ISM inferred from the regional tree ring $\delta^{18}O$ record

The results of spectral analysis using the multi-taper method (Mann and Lees, 1996) indicates that the H5 regional tree ring $\delta^{18}O$ record contains several high-frequency periodicities (4 and 5 years), as well as lower frequency periodicities (~133 years) at a confidence level greater than 99% (Figure 7). This indicates that interannual and centennial variability of the ISM was dominant characteristic feature during the last several hundred years. The interannual variability (4-5 years) of the H5 record is similar to that of ENSO, suggesting a possible relationship (Mason, 2001). The spatial correlation between the H5 record

and SST also reveals a close relationship between the ISM and ENSO (Figure 8). Other high-resolution ISM-related records from monsoonal Asia also exhibit similar inter-annual periodicities (Sun et al., 2016; Xu et al., 2013a; Yadava and Ramesh, 2007). In addition, meteorological data indicates that ENSO has had a significant influence on changes in the ISM change since 1870 CE (Kumar et al., 1999; Webster et al., 1998).

5

However, observational data indicate that the ENSO-ISM relationship is not consistent over time because of the southeastward shift of the descending limb of the Walker circulation and the varying monsoonal impact of the different patterns of El Niño (Kumar et al., 1999; Kumar et al., 2006). Thirty-one-year running correlations between the H5 regional tree ring $\delta^{18}O$ record and two reconstructed ENSO indices (McGregor et al., 2010; Wilson et al., 2006) reveal that this type of unstable ISM-ENSO
10 relationship occurred during the last 250 years (Figure 9). The reason may be that the two different patterns of El Niño (eastern-Pacific and central-Pacific) yield different monsoon impacts (Kumar et al., 2006). In addition, other factors, such as the Indian Ocean Dipole, also influence the ISM (Ashok et al., 2001; Abram et al., 2008).

Most proxy-based ENSO reconstructions focused on canonical El Niño events (eastern-Pacific El Niño) that are characterized
15 by unusually warm sea surface temperatures (SST) in the eastern equatorial Pacific (Gergis and Fowler, 2009; Li et al., 2011; McGregor et al., 2010); while a different type of El Nino (central-Pacific El Nino) is characterized by warm SSTs in the central Pacific, flanked by cooler SSTs to the west and east. The latter is termed El Niño Modoki or the central-Pacific El Niño (Ashok et al., 2007; Kao and Yu, 2009; Yeh et al., 2009), and it has a different effect on the ISM (Kumar et al., 2006). In order to characterize in detail the relationship between the ISM and the two types of ENSO during the last several hundred years, long-
20 term coral-based records from the tropical eastern and central Pacific are needed. However, such high-resolution, continuous and robust SST reconstructions are scarce. Even in the equatorial Pacific 'centre of action' (COA) of ENSO, the COA SST reconstruction is not considered robust prior to 1850 CE (Wilson et al., 2010). A new eastern Pacific SST record for the last

400 years is not reliable during the interval from 1635-1702 CE and 1840-1885 CE (Tierney et al., 2015). The future availability of longer, annually resolved marine records that provide independent estimates of SSTs in the tropical Pacific will improve our understanding of the relationship between the ISM and the two types of ENSO.

3.4 Centennial variability of the ISM inferred from the regional tree ring $\delta^{18}O$ record

There are also significant centennial-scale variations in the H5 record (Figure 7), which were extracted using a 100-year low-pass filter (Figure 10c, red line). The record exhibits a decreasing trend from 1743 to 1820 CE and an increasing trend since 1820 CE, which indicates a weakening trend of the ISM during the interval from 1820-2000 CE. A reduction in the monsoon precipitation/relative humidity of the ISM in the last 200 years is also evident in other areas influenced by the ISM. Maar lake sediments in Myanmar exhibit a decreasing trend of monsoonal rainfall since 1840 CE (Sun et al., 2016); a tree ring $\delta^{18}O$ record from southeast Asia exhibits a drying trend since 1800 CE (Xu et al., 2013a); a stalagmite $\delta^{18}O$ record from southwest China reveals an overall decreasing trend in monsoon precipitation since 1760 CE (Tan et al., 2016); and in southwest China, tree ring $\delta^{18}O$ and maar lake records indicate reduced monsoon precipitation/relative humidity/cloud cover since 1840 or 1860 CE (Chu et al., 2011; Grießinger et al., 2016; Liu et al., 2014; Wernicke et al., 2015; Xu et al., 2012). Monsoon precipitation in northwestern India shows a significant decreasing trend during the period of 1866-2006 (Bhutiyani et al., 2010).

However, in contrast, marine sediment records from the Western and Southeastern Arabian Sea exhibit an increasing trend of ISM strength over the last four centuries (Anderson et al., 2002; Chauhan et al., 2010). A recent study indicated that the contrasting trends in the ISM during the last several hundred years observed in geological records resulted from the different behavior of the Bay of Bengal branch and Arabian Sea branch of the ISM (Tan et al., 2016), and the Bay of Bengal branch of ISM weakened while intensity of Arabian Sea branch of the ISM increased during the last 200 years. However, the tree ring $\delta^{18}O$ record in northwest India, influenced by the Arabian Sea branch of the ISM, exhibits a drying trend since 1950 CE (Sano

et al., In press), which does not support the idea of a strengthening Arabian Sea branch of the ISM (Anderson et al., 2002). Moreover, there are no calibrated radiocarbon dates for the last 300 years for the two records from the Arabian Sea (Anderson et al., 2002a; Chauhan et al., 2010). We suggest that further high-resolution and well-dated ISM records from western India are needed to improve our understanding of the behavior of the ISM. Although reconstructed All India monsoon rainfall does not show a significant decreasing trend during the period of 1813-2005 (Sontakke et al., 2008), the data from only four stations extend back to 1826 CE and four longest stations locate in central or southern India. Monsoon season drying trend in northern India revealed by H5 regional tree ring $\delta^{18}O$ record may indicate that inland areas appear to be particularly sensitive to the weakening of monsoon circulation.

The H5 record suggests a decreasing trend of ISM strength, which is supported by most of the other well-dated and high-resolution ISM records in ISM margin areas. A previous study has indicated that solar irradiance has a significant influence on the ISM on multi-decadal to centennial timescales, and that reduced solar output is correlated with weaker ISM winds (Gupta et al., 2005). However, solar irradiance has increased since 1810-1820 CE (Bard et al., 2000; Lean et al., 1995) and therefore it cannot be the main reason for the weaker ISM since 1820 CE. Atmospheric CO_2 content is another forcing factor for the ISM, with higher atmospheric CO_2 content resulting in a stronger ISM (Kripalani et al., 2007; Meehl and Washington, 1993). Thus, the increased atmospheric CO_2 content during the last 200 years is unlikely to be the reason for the weakened ISM.

The land-sea thermal contrast which is also an important influencing factor for ISM (Roxy et al., 2015), is evaluated by atmospheric temperature gradient between the Tibetan Plateau and the tropical Indian Ocean (Fu and Fletcher, 1985; Sun et al., 2010). The history of land-sea thermal contrasts is reconstructed based on temperature differences between the Tibetan Plateau and the Indian Ocean (Figure 10a), and centennial variations of land-sea thermal contrasts are shown in Figure 10b.

Three reconstructed land-sea thermal contrasts showed a decreasing trend since 1800 CE and 1820 CE (Figure 10b), and the H5 record exhibits a similar pattern of changes on a centennial scale (Figure 10c). The decreasing land-sea thermal contrast since 1800 and 1820 CE has resulted in a weaker ISM, and the increasing trend of the H5 record since 1820 CE also indicates a reduced ISM intensity. In addition, aerosol emissions may be another reason to cause weakened ISM. Because the aerosol-induced differential cooling of the source and nonsource regions resulted in not only reduced local land-ocean surface thermal contrast but also weaken large-scale meridional atmospheric temperature gradients, both of which caused weakening Indian summer monsoon circulation (Bollasina et al., 2011; Cowan and Cai, 2011). Long-term aerosol emissions record is needed to evaluate aerosol emission's influences on ISM in the past.

3.5 Comparison of regional tree ring $\delta^{18}O$ record with speleothem $\delta^{18}O$ record in northern India

The H5 regional tree ring $\delta^{18}O$ record does not exhibit significant decadal to multi-decadal periodicities (Figure 7), while the main spectral component of high-resolution speleothem $\delta^{18}O$ records (a proxy of ISM rainfall in northern and central India) consists of multi-decadal periodicities (~15, 20, 30, 60 and 70 years) (Sinha et al., 2011; Sinha et al., 2015). This inconsistency may be the result of the different types of proxy record used together with micro-environmental differences between the sampling sites. Although decadal to multi-decadal variability of the H5 tree ring $\delta^{18}O$ record is not strongly developed, the record does contain decadal to multi-decadal changes. Decadal to multi-decadal variability was extracted using bandpass filters (15-80 years) (Figure 11, red line). From the perspective of decadal to multi-decadal changes, the H5 record shares similarities with the speleothem record, while the H5 record are out-of-phase with speleothem $\delta^{18}O$ records during several intervals (Figure 11).

Based on the oxygen isotope fractionation theory, tree ring $\delta^{18}O$ and speleothem $\delta^{18}O$ should share similar changes (Managave, 2014) if both of them inherit a common source water $\delta^{18}O$ signal, as shown by Ramesh et al. (2013). The following reasons

may cause incoherence between regional tree ring $\delta^{18}O$ and speleothem $\delta^{18}O$. Other controlling factors differentially affect tree ring $\delta^{18}O$ and speleothem $\delta^{18}O$ values. Relative humidity has an important impact on tree ring $\delta^{18}O$ (Roden et al., 2000). Lower relative humidity result in enhanced evaporative enrichment of leaf water and then higher tree ring cellulose $\delta^{18}O$, while the relative humidity may not affect speleothem $\delta^{18}O$ when relative humidity does not correlate with precipitation $\delta^{18}O$ (Managave, 2014). Model results show that relative humidity's influences on the correlation between tree ring $\delta^{18}O$ and speleothem $\delta^{18}O$ is more pronounced in the regions where the variation of relative humidity during the growing season exceeds 1% (Managave, 2014). In contrast, the cave epikarst dynamics affect speleothems $\delta^{18}O$ significantly (Lachniet, 2009). The infiltrating water from different rainfall events may be stored and mixed in the epikarst. Lag times of $\delta^{18}O$ values in drip waters relative to rainfall are several years or decades in some locations (Lachniet, 2009), and a slow transit time smoothed climate signal. These processes may result in different source water for tree ring and speleothem. In addition, limited three ^{230}Th dates points (3 control points) and relative large age uncertainty (9-31 years) of speleothems $\delta^{18}O$ time series during the common period of 1743-2000 may result in the incoherence between tree ring and speleothems $\delta^{18}O$. Long-term process-based study on tree ring $\delta^{18}O$ and speleothem $\delta^{18}O$ variations in future study are needed for a better understanding for climatic implication of two proxies.

4 Conclusions

We have combined three published tree ring cellulose $\delta^{18}O$ records (from Northwest India, western Nepal and Bhutan) with two new tree ring cellulose $\delta^{18}O$ records (from northern India and central Nepal) to produce a regional record (H5) for the northern Indian sub-continent for the interval from 1743-2008 CE. This record is significantly and negatively correlated with All India Rainfall (r = -0.5, p <0.001, n =138), the Indian monsoon index (r = -0.45, p <0.001, n =51) and the intensity of the monsoon circulation (r = -0.42, p <0.001, n =51). Spatial correlation analysis indicates that the H5 record is negatively correlated with June-September precipitation in the northern Indian sub-continent. The Indian summer monsoon (ISM)

controls the tree ring cellulose $\delta^{18}O$ record via its effects on the $\delta^{18}O$ of precipitation and relative humidity. Based on the observed statistical relationships and the physical mechanisms linking variations in tree ring $\delta^{18}O$ and the ISM, regional tree ring cellulose $\delta^{18}O$ chronology in the northern Indian sub-continent is a suitable high-resolution proxy for past ISM changes.

Inter-annual and centennial variations are evident in the regional tree ring $\delta^{18}O$ chronology. Significant correlations between inter-annual changes and the El Niño-Southern Oscillation (ENSO) indicate that the ISM was affected by ENSO; however, this relationship was not consistent in the past. A robust, high-resolution and continuous ENSO reconstruction from the 'centre of action' area of the Pacific would shed more light on this relationship. Centennial-scale variations in the H5 record reveal a trend of weakened ISM intensity since 1820 CE, which is also evident in various high-resolution ISM records from southwest China and Southeast Asia. Reduced land-ocean contrasts since 1820 CE, together with increased anthropogenic aerosol emissions during the last hundred years, may have contributed to the weakened ISM.

Data availability:

The tree ring cellulose oxygen isotope data in this paper are available from NOAA Paleoclimatology Datasets (https://www.ncdc.noaa.gov/data-access/paleoclimatology-data). Hulma $\delta^{18}O$ chronology should be available at this link: https://www.ncdc.noaa.gov/paleo/study/22547 (Sano et al., 2017a), which was described by Sano et al. (2012).; Wache $\delta^{18}O$ chronology should be available at this link: https://www.ncdc.noaa.gov/paleo/study/22548 (Sano et al., 2017b), which was described by Sano et al. (2013); Manali $\delta^{18}O$ chronology should be available at this link: https://www.ncdc.noaa.gov/paleo/study/22549 (Sano et al., 2017c), which was described by Sano et al. (in press); JG $\delta^{18}O$ chronology should be available at this link: https://www.ncdc.noaa.gov/paleo/study/22550 (Xu et al., 2017a); Ganesh $\delta^{18}O$ chronology should be available at this link: https://www.ncdc.noaa.gov/paleo/study/22551 (Xu et al., 2017b).

Acknowledgments:

This work was jointly funded by the Ministry of Science and Technology of the People's Republic of China (Grant No. 2016YFA0600502), the Chinese Academy of Sciences (CAS) Pioneer Hundred Talents Program, the National Natural Science Foundation of China (Grant No. 41672179, 41630529 and 41430531), an environmental research grant from the Sumitomo Foundation, Japan, a research grant from the Research Institute of Humanity and Nature, Kyoto, Japan, and grant in-aid from the Japan Society for the Promotion of Science Fellows (23242047 and 23-10262). Indian Space Research Organization's Geosphere Biosphere Programme supported RR and APD. This study was conducted in the framework of the Past Global Changes (PAGES) Asia2k programme. We deeply appreciate the helpful comments from three anonymous reviewers, the editor and the group members of SPATIAL laboratory at the University of Utah to improve the manuscript.

References:

Abram, N. J., Gagan, M. K., Cole, J. E., Hantoro, W. S., and Mudelsee, M.: Recent intensification of tropical climate variability in the Indian Ocean, Nature Geoscience, 1, 849-853, 2008.

Anderson, D. M., Overpeck, J. T., and Gupta, A. K.: Increase in the Asian southwest monsoon during the past four centuries, Science, 297, 596-599, 2002.

Ashok, K., Behera, S. K., Rao, S. A., Weng, H., and Yamagata, T.: El Niño Modoki and its possible teleconnection, Journal of Geophysical Research: Oceans (1978-2012), 112, 2007.

Ashok, K., Guan, Z., and Yamagata, T.: Impact of the Indian Ocean dipole on the relationship between the Indian monsoon rainfall and ENSO, Geophysical Research Letters, 28(23), 4499-4502, 2001.

Bard, E., Raisbeck, G., Yiou, F., and Jouzel, J.: Solar irradiance during the last 1200 years based on cosmogenic nuclides, Tellus Series B-chemical & Physical Meteorology, 52, 985-992, 2000.

Bhutiyani, M. R., Kale, V. S., and Pawar, N J: Climate change and the precipitation variations in the northwestern Himalaya:

1866-2006, International Journal of Climatology, 30(4), 535-548, 2010.

Bollasina, M. A. and Ramaswamy, V.: Anthropogenic Aerosols and the Weakening of the South Asian Summer Monsoon, Science, 334, 502-505, 2011.

Cai, Z. and Tian, L.: Atmospheric Controls on Seasonal and Interannual Variations in the Precipitation Isotope in the East Asian Monsoon Region, Journal of Climate, 29, 1339-1352, 2016.

Chauhan, O. S., Dayal, A. M., Nathani, B., and Abdul, K. U. S.: Indian summer monsoon and winter hydrographic variations over past millennia resolved by clay sedimentation, Geochemistry Geophysics Geosystems, 11, 633-650, 2010.

Cook, E., Krusic, P., Anchukaitis. K., Buckley, M., Nakatsuka, T., Sano, M., and PAGES Asia2k Members: Tree-ring reconstructed summer temperature anomalies for temperate East Asia since 800 CE. Climate Dynamics, 41, 2957-2972, 2013.

Cook, E., Krusic, P., Anchukaitis. K., Buckley, M., Nakatsuka, T., Sano, M., and PAGES Asia2k Members: Asia 1200 Year Gridded Summer Temperature Reconstructions, World Data Center for Paleoclimatology, https://www.ncdc.noaa.gov/paleo-search/study/19523, 2013.

Cowan, T., Cai, W.: The impact of Asian and non-Asian anthropogenic aerosols on 20th century Asian summer monsoon, Geophysical Research Letters, 38, 417-417, 2011.

Chu, G., Sun, Q., Yang, K., Li, A., Yu, X., Xu, T., Yan, F., Wang, H., Liu, M., and Wang, X.: Evidence for decreasing South Asian summer monsoon in the past 160 years from varved sediment in Lake Xinluhai, Tibetan Plateau, Journal of Geophysical Research, 116, D02116, 2011.

Dansgaard, W.: Stable isotopes in precipitation, Tellus, 16, 436-468, 1964.

Duan, K., Yao, T., and Thompson, L. G.: Low-frequency of southern Asian monsoon variability using a 295-year record from the Dasuopu ice core in the central Himalayas (SCI), Geophysical Research Letters, 31, 371-375, 2004.

Fan, F., Mann, M. E., and Ammann, C. M.: Understanding Changes in the Asian Summer Monsoon over the Past Millennium:

Insights from a Long-Term Coupled Model Simulation*, Journal of Climate, 22, 1736-1748, 2009.

Fu, C. and Fletcher, J.: The Relationship between Tibet-Tropical Ocean Thermal Contrast and Interannual Variability of Indian Monsoon Rainfall. Journal of Applied Meteorology, 24(8), 841-848, 1985.

Gagen, M., McCarroll, D., Loader, N. J., and Robertson, I.: Stable Isotopes in Dendroclimatology: Moving Beyond 'Potential', Dendroclimatology, 2011. 147-172, 2011.

Gergis, J. L. and Fowler, A. M.: A history of ENSO events since AD 1525: implications for future climate change, Climatic change, 92, 343-387, 2009.

Goswami, B. N., Madhusoodanan, M. S., Neema, C. P., and Sengupta, D.: A physical mechanism for North Atlantic SST influence on the Indian summer monsoon, Geophysical Research Letters, 33, 356-360, 2006.

Green, J.: Methods in carbohydrate chemistry, Whistler RL, Green JW, 1963. 1963.

Grießinger, J., Bräuning, A., Helle, G., Hochreuther, P., and Schleser, G.: Late Holocene relative humidity history on the southeastern Tibetan plateau inferred from a tree-ring $\delta^{18}O$ record: Recent decrease and conditions during the last 1500 years, Quaternary International, 2016. 2016.

Gupta, A. K., Moumita, D., and Anderson, D. M.: Solar influence on the Indian summer monsoon during the Holocene, Geophysical Research Letters, 32, 261-261, 2005.

Hiremath, K. M., Manjunath, H., and Soon, W.: Indian summer monsoon rainfall: Dancing with the tunes of the sun, New Astronomy, 35, 8-19, 2015.

Holmes, R.: Computer-assisted quality control in tree-ring dating and measurement, Tree-ring bulletin, 43, 69-78, 1983.

Kagawa, A., Sano, M., Nakatsuka, T., Ikeda, T., and Kubo, S.: An optimized method for stable isotope analysis of tree rings by extracting cellulose directly from cross-sectional laths, Chemical Geology, s393–394, 16-25, 2015.

Kao, H.-Y. and Yu, J.-Y.: Contrasting eastern-Pacific and central-Pacific types of ENSO, Journal of Climate, 22, 615-632, 2009.

Kripalani, R., Oh, J., Kulkarni, A., Sabade, S., and Chaudhari, H.: South Asian summer monsoon precipitation variability:

Coupled climate model simulations and projections under IPCC AR4, Theoretical and Applied Climatology, 90, 133-159, 2007.

Kumar, K. K., Rajagopalan, B., and Cane, M. A.: On the weakening relationship between the Indian monsoon and ENSO, Science, 284, 2156-2159, 1999.

Kumar, K. K., Rajagopalan, B., Hoerling, M., Bates, G., and Cane, M.: Unraveling the mystery of Indian monsoon failure during El Niño, Science, 314, 115-119, 2006.

Lachniet, M. S.: Climatic and environmental controls on speleothem oxygen-isotope values. Quaternary Science Reviews, 28(5–6), 412-432, 2009.

Lean, J., Beer, J., and Bradley, R.: Reconstruction of solar irradiance since 1610: Implications for climate change, Geophysical Research Letters, 22, 3195-3198, 1995.

Lekshmy, P.R., Ramesh, R., Midhun, M., and Jani, R.A.: ^{18}O depletion in monsoon rain relates to large scale convection rather than the amount of rainfall, Scientific reports,4.5661, doi:10.1038/srepo5661, 2014.

Lekshmy, P.R., Midhun, M., and Ramesh, R.: Spatial variation of amount effect over peninsular India and Sri Lanka: role of seasonality, Gephys. Res. Lett., 42, 5500-5507, doi:10.1002/2015GL064517, 2015.

Li, J., Xie, S. P., Cook, E. R., Huang, G., D'Arrigo, R., Liu, F., Ma, J., and Zheng, X. T.: Interdecadal modulation of El Niño amplitude during the past millennium, Nature Climate Change, 1, 114-118, 2011.

Liu, X., Xu, G., Grießinger, J., An, W., Wang, W., Zeng, X., Wu, G., and Qin, D.: A shift in cloud cover over the southeastern Tibetan Plateau since 1600: evidence from regional tree-ring δ 18 O and its linkages to tropical oceans, Quaternary Science Reviews, 88, 55-68, 2014.

Loader, N., Robertson, I., Barker, A., Switsur, V., and Waterhouse, J.: An improved technique for the batch processing of small wholewood samples to α-cellulose, Chemical Geology, 136, 313-317, 1997.

Managave, S. R.: Model evaluation of the coherence of a common source water oxygen isotopic signal recorded by tree-ring

cellulose and speleothem calcite, Geochemistry Geophysics Geosystems, 15, 905–922, 2014.

Mann, M. E. and Lees, J. M.: Robust estimation of background noise and signal detection in climatic time series, Climatic change, 33, 409-445, 1996.

Mason, S. J.: El Niño, climate change, and Southern African climate, Environmetrics, 12, 327-345, 2001.

McGregor, S., Timmermann, A., and Timm, O.: A unified proxy for ENSO and PDO variability since 1650, Climate of the Past, 6, 1-17, 2010.

McGregor, S., Timmermann, A., and Timm, O.: A unified proxy for ENSO and PDO variability since 1650, World Data Center for Paleoclimatology, https://www.ncdc.noaa.gov/paleo-search/study/8732, 2010

Meehl, G. A. and Washington, W. M.: South asian summer monsoon variability in a model with doubled atmospheric carbon dioxide concentration, Science, 260, 1101-1104, 1993.

Mooley, D. A. and Parthasarathy, B.: Fluctuations in All-India summer monsoon rainfall during 1871–1978, Climatic Change, 6, 287-301, 1984.

Mooley, D., Parthasarathy, B., Kumar, K., Sontakke, N., Munot, A., and Kothawale, D. Indian Institute of Tropical Meteorology Homogeneous Indian Monthly Rainfall Data Sets (1871-2014), http://www.tropmet.res.in/static_page.php?page_id=53, 2016

Naidu, C. V., Durgalakshmi, K., Krishna, K. M., Rao, S. R., Satyanarayana, G. C., Lakshminarayana, P., and Rao, L. M.: Is summer monsoon rainfall decreasing over India in the global warming era?, Journal of Geophysical Research Atmospheres, 114, 144-153, 2009.

Ramesh, R., Bhattacharya, S.K. And Gopalan, K.: Climatic correlations of the stable isotope records of silver fir (*Abies pindrow*) trees from Kashmir, India. Earth and Planetary Science Letters, 79, 66-74, 1986.

Ramesh, R., Mangave, S.R. and Yadava, M.G.: Paleoclimates of Peninsular India, in “Climate Change and Island and Coastal Vulnerability”. Capital Publishing Company, New Delhi (eds. Sundaresan J., et al.). pp.78-100, 2013.

Risi, C., Bony, S., and Vimeux, F.: Influence of convective processes on the isotopic composition ($\delta^{18}O$ and δD) of precipitation and water vapor in the tropics: 2. Physical interpretation of the amount effect, Journal of Geophysical Research: Atmospheres (1984-2012), 113, 2008.

Roden, J. S., Lin, G., and Ehleringer, J. R.: A mechanistic model for interpretation of hydrogen and oxygen isotope ratios in tree-ring cellulose, Geochimica et Cosmochimica Acta, 64, 21-35, 2000.

Roxy, M.K., Ritika, K., Terray, P., Murtugudde,R., Ashok, K., and Goswami, B.N.: Drying of Indian subcontinent by rapid Indian Ocean warming and a weakening land-sea thermal gradient, Nature Communications, 6:7423, doi:10.1038/ncomms8423, 2015.

Sano, M., Ramesh, R., Sheshshayee, M., and Sukumar, R.: Increasing aridity over the past 223 years in the Nepal Himalaya inferred from a tree-ring $\delta^{18}O$ chronology, The Holocene, 1-9. 2011.

Sano, M., Ramesh, R., Sheshshayee, M., and Sukumar, R.: Tree ring oxygen isotope chronology in western Nepal, World Data Center for Paleoclimatology, https://www.ncdc.noaa.gov/paleo/study/22547, 2017a.

Sano, M., Tshering, P., Komori, J., Fujita, K., Xu, C., and Nakatsuka, T.: May–September precipitation in the Bhutan Himalaya since 1743 as reconstructed from tree ring cellulose $\delta^{18}O$, Journal of Geophysical Research: Atmospheres, 118, 8399-8410, 2013.

Sano, M., Tshering, P., Komori, J., Fujita, K., Xu, C., and Nakatsuka, T.: Tree ring oxygen isotope chronology in Bhutan, World Data Center for Paleoclimatology, https://www.ncdc.noaa.gov/paleo/study/22548, 2017b.

Sano, M., Dimri, A.P., Ramesh, R., Xu, C., Li, Z., and Nakatsuka, T.: Moisture source signals preserved in a 242-year tree-ring $\delta^{18}O$ chronology in the western Himalaya, Global and Planetary Change, In press.

Sano, M., Dimri, A., Ramesh, R., Xu, C., Li, Z., and Nakatsuka T.: Tree ring oxygen isotope chronology in Northwest India, World Data Center for Paleoclimatology, https://www.ncdc.noaa.gov/paleo/study/22549, 2017c.

Shi, F., Ge, Q., Bao, Y., Li, J., Yang, F., Ljungqvist, F. C., Solomina, O., Nakatsuka, T., Wang, N., and Zhao, S.: A multi-proxy

reconstruction of spatial and temporal variations in Asian summer temperatures over the last millennium, Climatic Change, 131, 663-676, 2015.

Shi, F., Ge, Q., Bao, Y., Li, J., Yang, F., Ljungqvist, F. C., Solomina, O., Nakatsuka, T., Wang, N., and Zhao, S.: Asian 1,100 Year Multiproxy Gridded Summer Temperature Reconstructions, World Data Center for Paleoclimatology, http://ncdc.noaa.gov/paleo/study/18635, 2015.

Sinha, A., Berkelhammer, M., Stott, L., Mudelsee, M., Cheng, H., and Biswas, J.: The leading mode of Indian Summer Monsoon precipitation variability during the last millennium, Geophysical Research Letters, 38, 532-560, 2011.

Sinha, A., Kathayat, G., Cheng, H., Breitenbach, S. F. M., Berkelhammer, M., Mudelsee, M., Biswas, J., and Edwards, R. L.: Trends and oscillations in the Indian summer monsoon rainfall over the last two millennia, Nat Commun, 6, 2015.

Sinha, A., Kathayat, G., Cheng, H., Breitenbach, S. F. M., Berkelhammer, M., Mudelsee, M., Biswas, J., and Edwards, R. L.: Trends and oscillations in the Indian summer monsoon rainfall over the last two millennia, Supplementary Data 2, Nat Commun, 6, 2015.

Sontakke, N. A., Singh, N., and Singh, H. N.: Instrumental period rainfall series of the Indian region (AD1813–2005): revised reconstruction, update and analysis, Holocene, 18(7), 1055-1066, 2008.

Sun, Q., Shan, Y., Sein, K., Su, Y., Zhu, Q., Wang, L., Sun, J., Gu, Z., and Chu, G.: A 530-year-long record of the Indian Summer Monsoon from carbonate varves in Maar Lake Twintaung, Myanmar, Journal of Geophysical Research Atmospheres, 2016. 2016.

Sun, Y., Ding, Y., and Dai, A: Changing links between South Asian summer monsoon circulation and tropospheric land-sea thermal contrasts under a warming scenario. Geophysical Research Letters, 37(2), 195-205, 2010.

Tan, L., Cai, Y., An, Z., Cheng, H., Shen, C. C., Gao, Y., and Edwards, R. L.: Decreasing monsoon precipitation in southwest China during the last 240 years associated with the warming of tropical ocean, Climate Dynamics, 2016. 1-10, 2016.

Tierney, J. E., Abram, N. J., Anchukaitis, K. J., Evans, M. N., Cyril, G., Halimeda, K. K., Saenger, C. P., Wu, H. C., and Jens,

Z.: Tropical sea surface temperatures for the past four centuries reconstructed from coral archives, Paleoceanography, 30, 226-252, 2015.

Tierney, J., Abram, N., Anchukaitis, K., Evans, M., Cyril, G., Halimeda, K., and Saenger, C., PAGES Ocean2K 400 Year Coral Data and Tropical SST Reconstructions, World Data Center for Paleoclimatology, https://www.ncdc.noaa.gov/paleo-search/study/17955, 2015.

Vuille, M., Bradley, R., Werner, M., Healy, R., and Keimig, F.: Modeling $\delta^{18}O$ in precipitation over the tropical Americas: 1. Interannual variability and climatic controls, Journal of Geophysical Research, 108, 4174, 2003.

Vuille, M., Werner, M., Bradley, R., and Keimig, F.: Stable isotopes in precipitation in the Asian monsoon region, Journal of Geophysical Research, 110, D23108, 2005.

Wang, B., Wu, R., and Lau, K.: Interannual Variability of the Asian Summer Monsoon: Contrasts between the Indian and the Western North Pacific-East Asian Monsoons, Journal of Climate, 14, 4073-4090, 2001.

Wang, B., Wu, R., and Lau, K., Indian monsoon index, http://apdrc.soest.hawaii.edu/projects/monsoon/definition.html, 2001

Wang, J., Yang, B., Ljungqvist, F.: A Millennial Summer Temperature Reconstruction for the Eastern Tibetan Plateau from Tree-Ring Width, Journal of Climate, 28, 5289-5304, 2015.

Wang, J., Yang, B., and Ljungqvist, F.: Eastern Tibetan Plateau 1000 Year Summer Temperature Reconstruction, World Data Center for Paleoclimatology, https://www.ncdc.noaa.gov/paleo-search/study/20590, 2015.

Webster, P. J., Magaña, V. O., Palmer, T. N., Shukla, J., and Tomas, R. A.: Monsoons: Processes, predictability, and the prospects for prediction, Journal of Geophysical Research, 103, 14451-14510, 1998.

Webster, P. J. and Yang, S.: Monsoon and ENSO: Selectively interactive systems, Quarterly Journal of the Royal Meteorological Society, 118, 877-926, 1992.

Wernicke, J., Grießinger, J., Hochreuther, P., and Bräuning, A.: Variability of summer humidity during the past 800 years on the eastern Tibetan Plateau inferred from $\delta^{18}O$ of tree-ring cellulose, Climate of the Past, 11, 327-337, 2015.

Wilson, R., Cook, E., D'Arrigo, R., Riedwyl, N., Evans, M. N., Tudhope, A., and Allan, R.: Reconstructing ENSO: the influence of method, proxy data, climate forcing and teleconnections, Journal of Quaternary Science, 25, 62-78, 2010.

Wilson, R., Tudhope, A., Brohan, P., Briffa, K., Osborn, T., and Tett, S.: Two-hundred-fifty years of reconstructed and modeled tropical temperatures, Journal of Geophysical Research, 111, C10007, 2006.

Wilson, R., Tudhope, A., Brohan, P., Briffa, K., Osborn, T., and Tett, S.: Coral-based Tropical Sea Surface Temperature Reconstruction, World Data Center for Paleoclimatology, https://www.ncdc.noaa.gov/paleo-search/study/6359, 2006.

Xu, C., Sano, M., and Nakatsuka, T.: A 400-year record of hydroclimate variability and local ENSO history in northern Southeast Asia inferred from tree-ring $\delta^{18}O$, Palaeogeography, Palaeoclimatology, Palaeoecology, 386, 588–598. 2013a.

Xu, C., Sano, M., and Nakatsuka, T.: Tree ring cellulose $\delta^{18}O$ of Fokienia hodginsii in northern Laos: A promising proxy to reconstruct ENSO?, Journal of Geophysical Research, 116, D24109, 2011.

Xu, C., Sano, M., Dimri, A.P., Ramesh, R., Nakatsuka, T., Shi, F., and Guo, Z.: Tree ring oxygen isotope chronology in northern India, World Data Center for Paleoclimatology, https://www.ncdc.noaa.gov/paleo/study/22550, 2017a.

Xu, C., Sano, M., Dimri, A.P., Ramesh, R., Nakatsuka, T., Shi, F., and Guo, Z.: Tree ring oxygen isotope chronology in central Nepal, World Data Center for Paleoclimatology, https://www.ncdc.noaa.gov/paleo/study/22551, 2017b.

Xu, C., Zheng, H., Nakatsuka, T., and Sano, M.: Oxygen isotope signatures preserved in tree ring cellulose as a proxy for April–September precipitation in Fujian, the subtropical region of southeast China, Journal of Geophysical Research, 118, 12,805-12,815, 2013b.

Xu, H., Hong, Y., and Hong, B.: Decreasing Asian summer monsoon intensity after 1860 AD in the global warming epoch, Climate dynamics, 2012. 1-10, 2012.

Yadav, R. R., Braeuning, A., and Singh, J.: Tree ring inferred summer temperature variations over the last millennium in western Himalaya, India, Climate Dynamics, 36, 1545-1554, 2011.

Yadava M.G. and Ramesh, R.: Significant longer-term periodicities in the proxy record of the Indian Mmonsoon rainfall, New

Astronomy,12, 544-555, 2007.

Yang, H., Johnson, K. R., Griffiths, M. L., and Yoshimura, K.: Interannual controls on oxygen isotope variability in Asian monsoon precipitation and implications for paleoclimate reconstructions: Oxygen Isotopes of Asian Monsoon Precipition, Journal of Geophysical Research Atmospheres, 121, 8410-8428. 2016.

Yeh, S.-W., Kug, J.-S., Dewitte, B., Kwon, M.-H., Kirtman, B. P., and Jin, F.-F.: El Niño in a changing climate, Nature, 461, 511-514, 2009.

Table 1. Tree ring cellulose oxygen isotope data sets used in this study

No.	Sample ID	Location	Period	Tree species	Mean	Climatic response of tree ring $\delta^{18}O$	Data source	Data Citations
1	Manali	32˚13′N, 77˚13′E, 2700 masl, India	1768-2008	*Abies pindrow*	29.97‰	Regional JJAS PDSI *r* =-0.67	Sano et al., In press	Sano et a 2017c
2	JG	29°38′N, 79°51′E, 3849 masl, India	1641-2008	*Cedrus deodara*	30.39‰	Regional JJAS PDSI *r* =-0.50	This study	Xu et a 2017a
3	Hulma	29°51′N, 81°56′E, 3850 masl, Nepal	1778–2000	*Abies spectabilis*	25.94‰	Regional JJAS PDSI *r* =-0.73	Sano et al., 2012	Sano et a 2017a
4	Ganesh	28°10′N, 85°11′E, 3550 masl, Nepal	1801-2000	*Abies spectabilis*	23.01‰	Regional JJAS PDSI *r* =-0.55	This study	Xu et a 2017b
5	Wache	27°59′N, 90°00′E, 3500 masl, Bhutan	1743-2011	*Larix griffithii*	19.38‰	Regional JJAS PDSI *r* =-0.59	Sano et al., 2013	Sano et a 2017b

Table 2: Correlation coefficients between the tree ring $\delta^{18}O$ records from different sampling locations

R (annual)	Manali	JG	Hulma	Ganesh
JG	0.50*			
Hulma	0.52*	0.51*		
Ganesh	0.47*	0.66*	0.61*	
Wache	0.23*	0.26*	0.37*	0.52*

R (multi-decadal)	Manali	JG	Hulma	Ganesh
JG	0.36*			
Hulma	0.37*	0.64*		
Ganesh	-0.03	0.94*	0.66*	
Wache	0.11	0.39*	0.38*	0.70*

*$p<0.01$

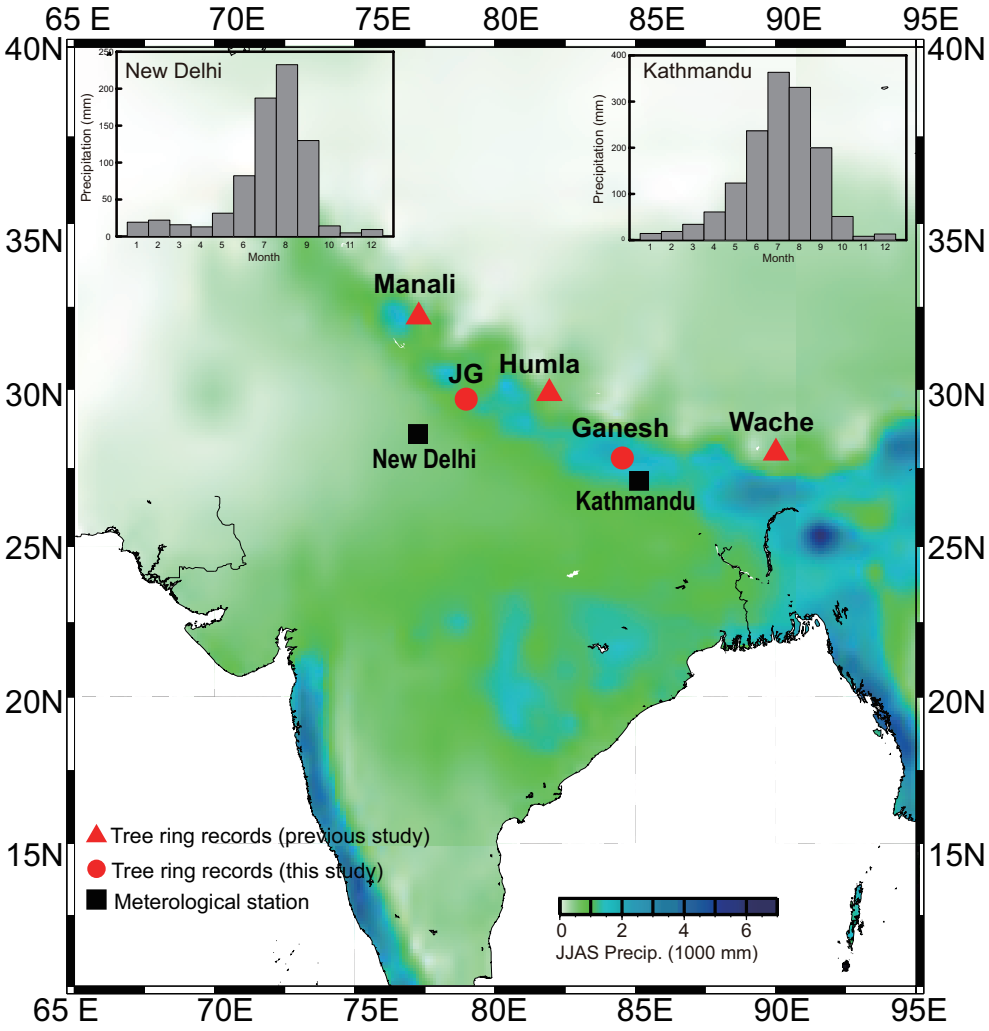

Figure 1. Map of the subcontinent showing tree-ring sites and color coded climatological monsoon precipitation from June to September. Insets show climatology of monthly precipitation at Kathmandu and New Delhi.

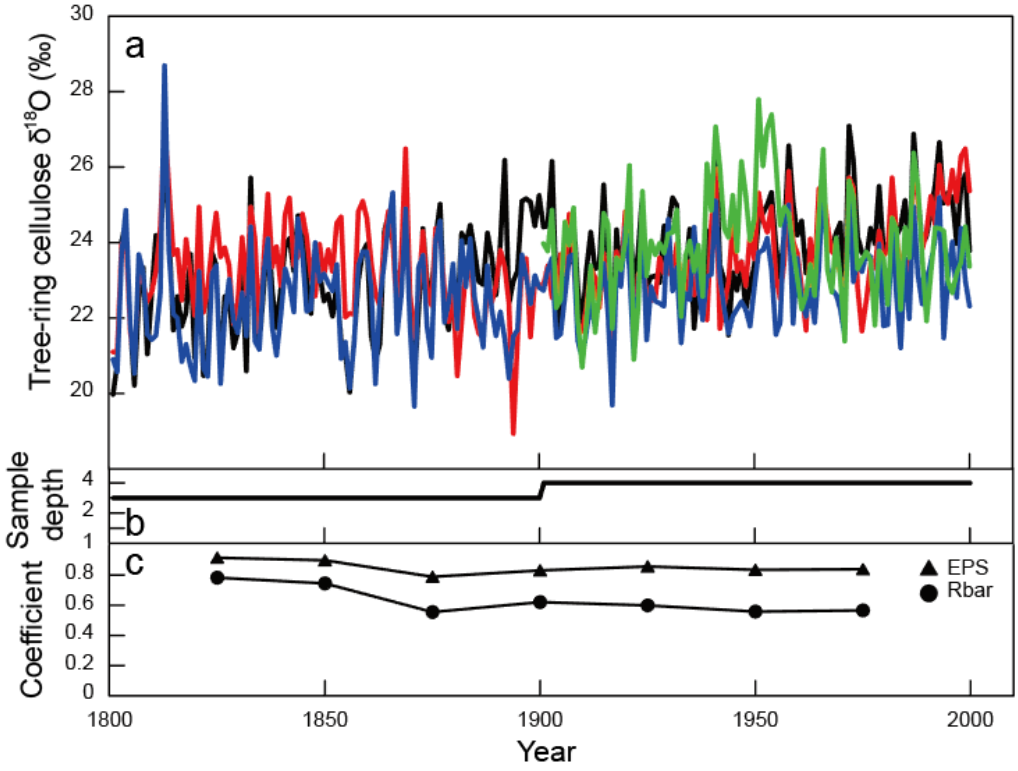

Figure 2. a: Tree ring $\delta^{18}O$ series of four individual trees: b: age profile, c: running EPS and Rbar statistics used 50-year windows and a 25-year lag for samples near Ganesh, Nepal.

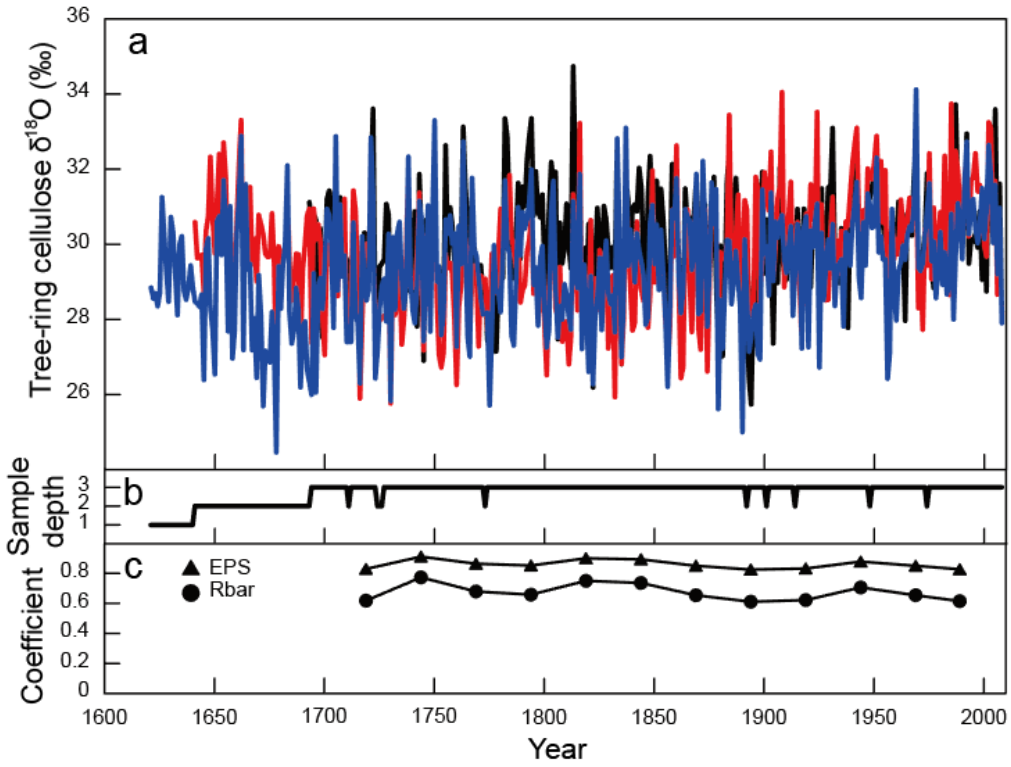

Figure 3. a: Tree ring $\delta^{18}O$ series for three individual trees: b: Age profile, c: running EPS and Rbar statistics using 50-year windows and a 25-year lag for samples near Jageshwar, India.

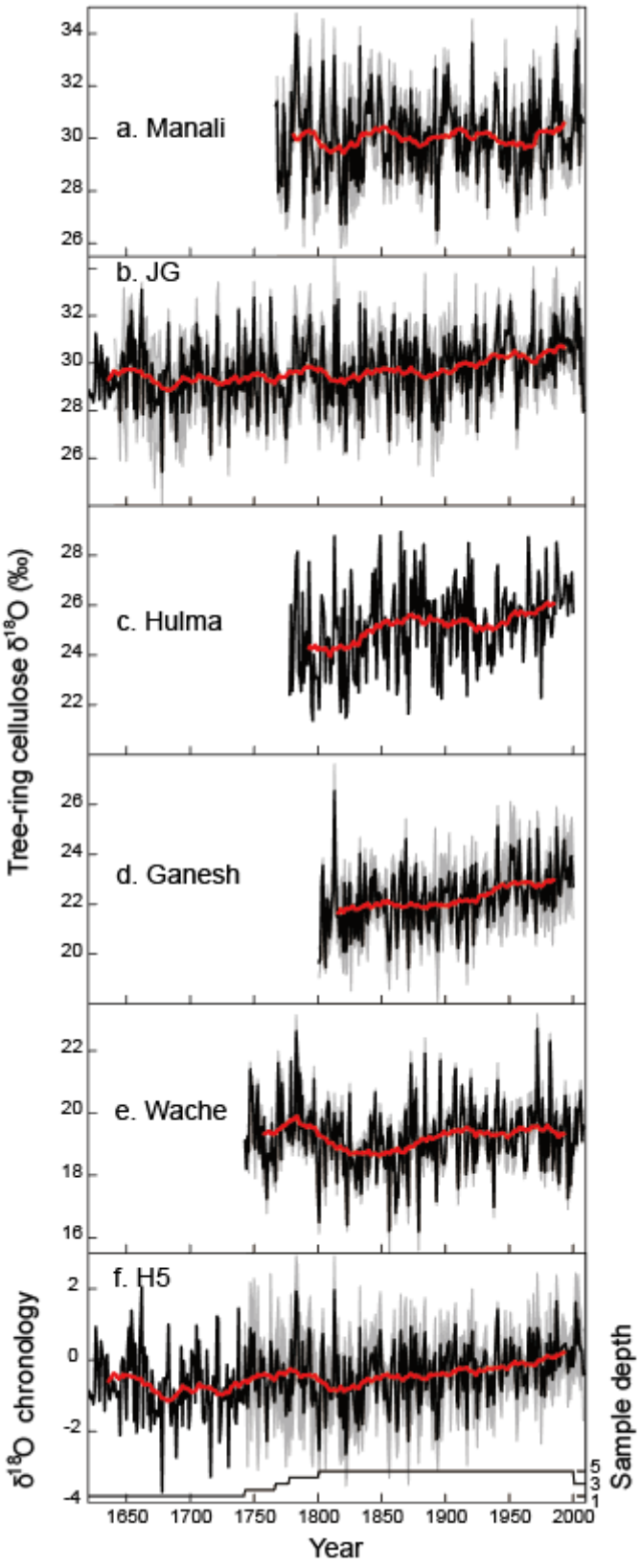
a. Manali
b. JG
c. Hulma
d. Ganesh
e. Wache
f. H5
Tree-ring cellulose δ18O (‰)
δ18O chronology
Sample depth
Year
1650
1700
1750
1800
1850
1900
1950
2000

Figure 4: Tree ring oxygen isotope chronologies from five sites (a-e) and the regional tree ring oxygen isotope chronology (f). (black line: mean values for all samples; red line: 31-year running average for the chronology; gray shadows: the 95% (±1.96σ) confidence limits)

5

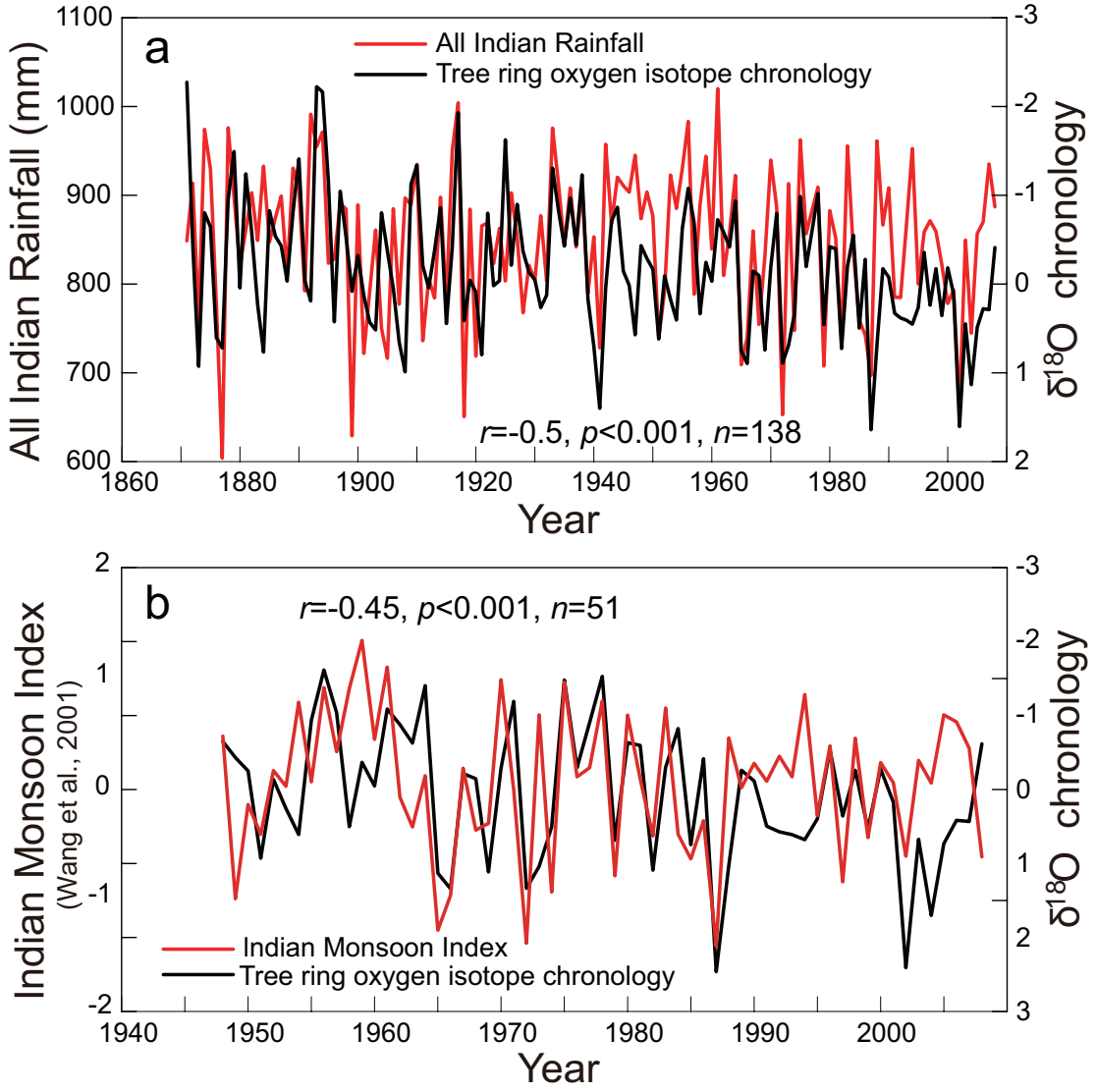

Figure 5. Comparison of the H5 regional tree ring $\delta^{18}O$ chronology with the All India Rainfall (a) and Indian Monsoon Index (b).

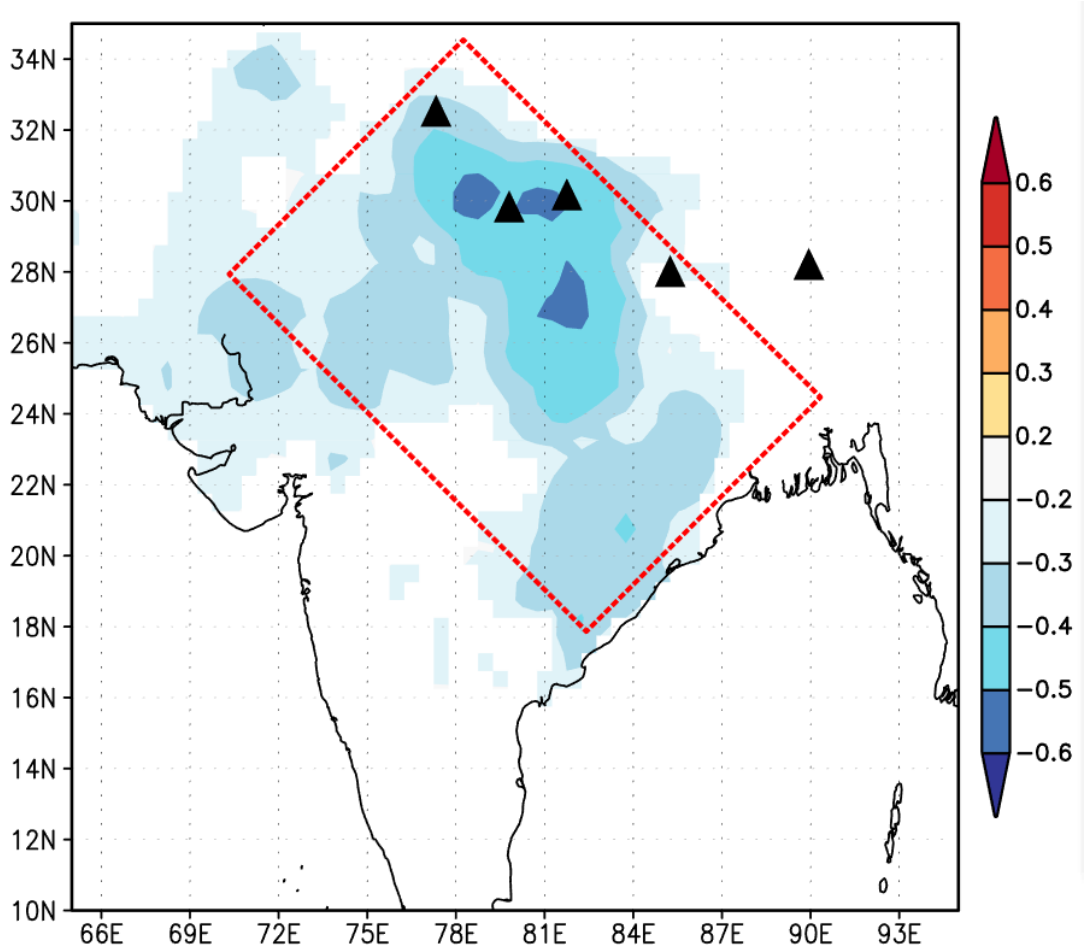

Figure 6. Spatial correlations between the H5 regional tree ring $\delta^{18}O$ record with June-September precipitation from GPCC V7 over interval from 1901-2008 CE. Only correlations significant at the 95% level are shown.

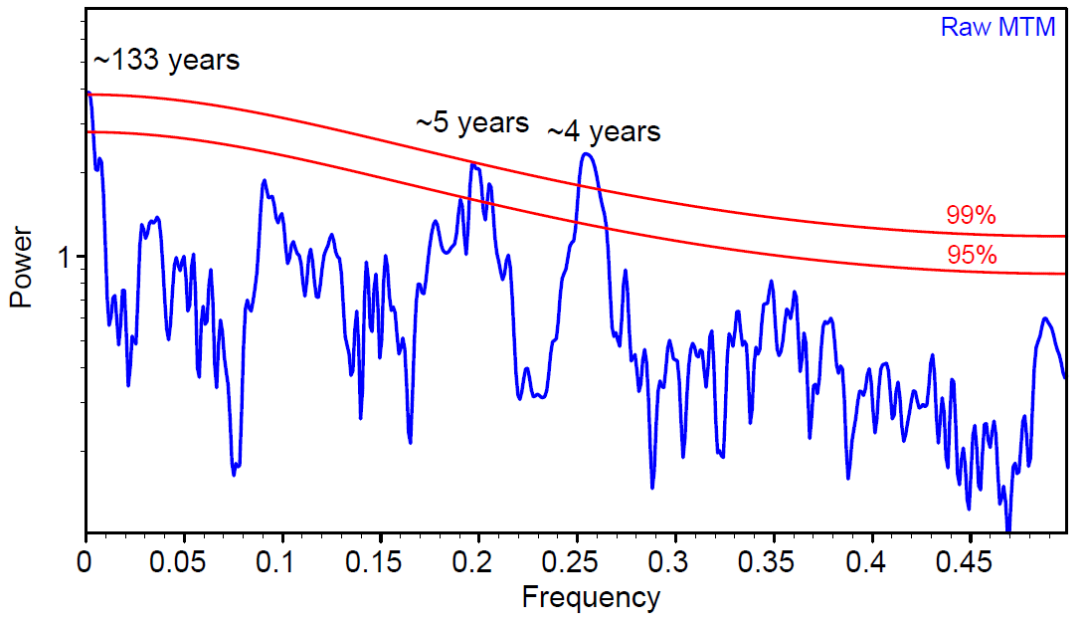

Figure 7. Multi-taper power spectra for the H5 regional tree ring $\delta^{18}O$ record.

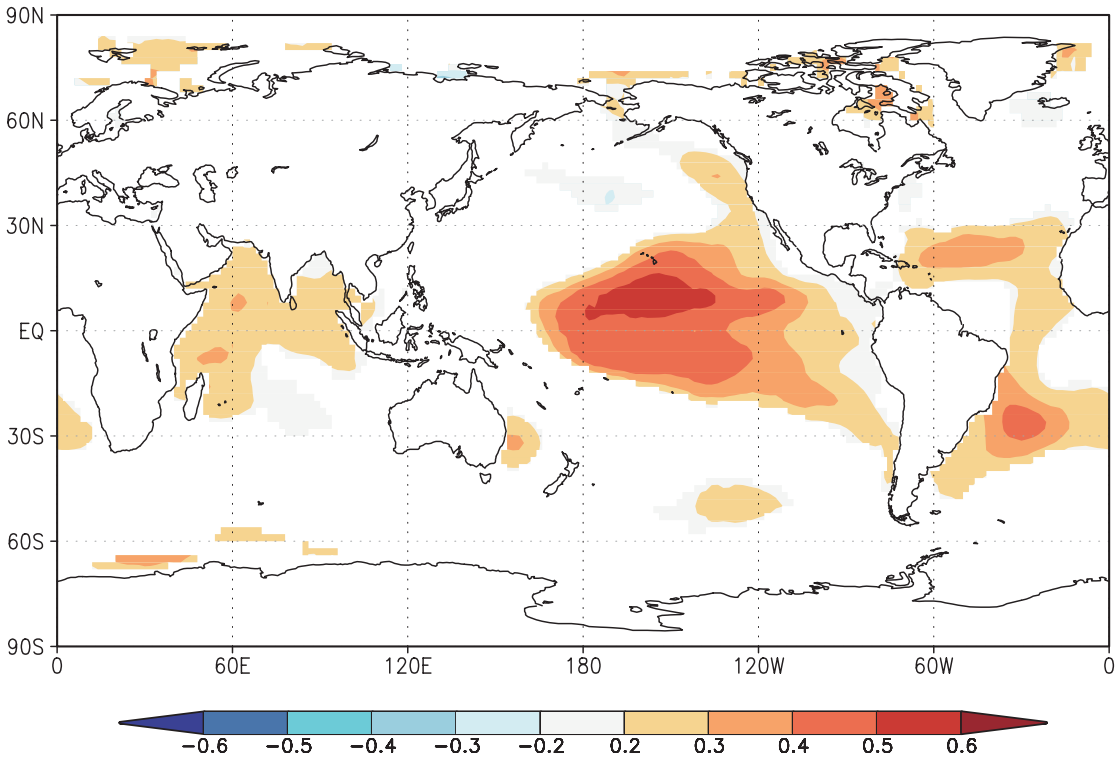

Figure 8. Spatial correlations between the H5 regional tree ring $\delta^{18}O$ record with May-September SST over the interval from 1871-2008 CE. Only correlations significant at the 95% level are shown.

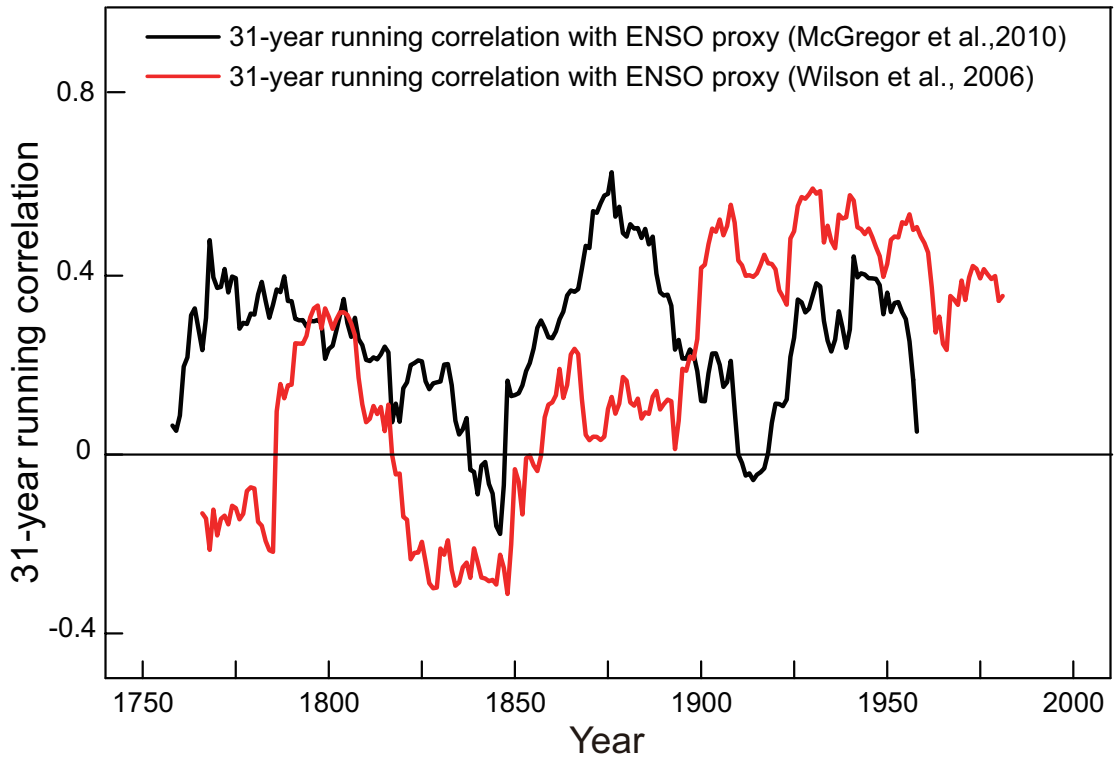

Figure 9. 31-year running correlation between the H5 regional tree ring $\delta^{18}O$ record and two reconstructed ENSO indices.

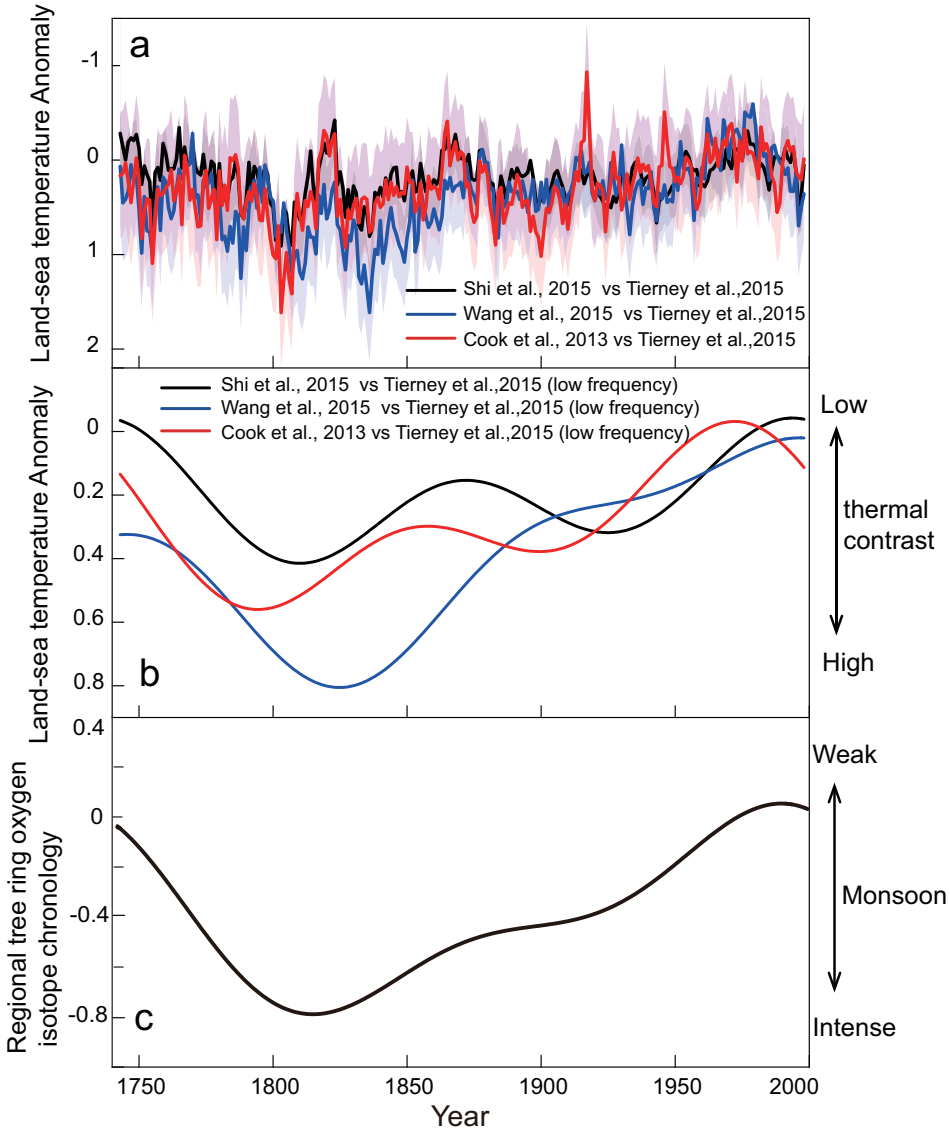

Figure 10. a: Land-sea Temperature Anomaly based on three summer temperature reconstruction for the Tibetan Plateau and one Indian Ocean SST reconstruction; b and c: centennial variations of land-sea thermal contrasts and the H5 regional tree ring $\delta^{18}O$ chronology.

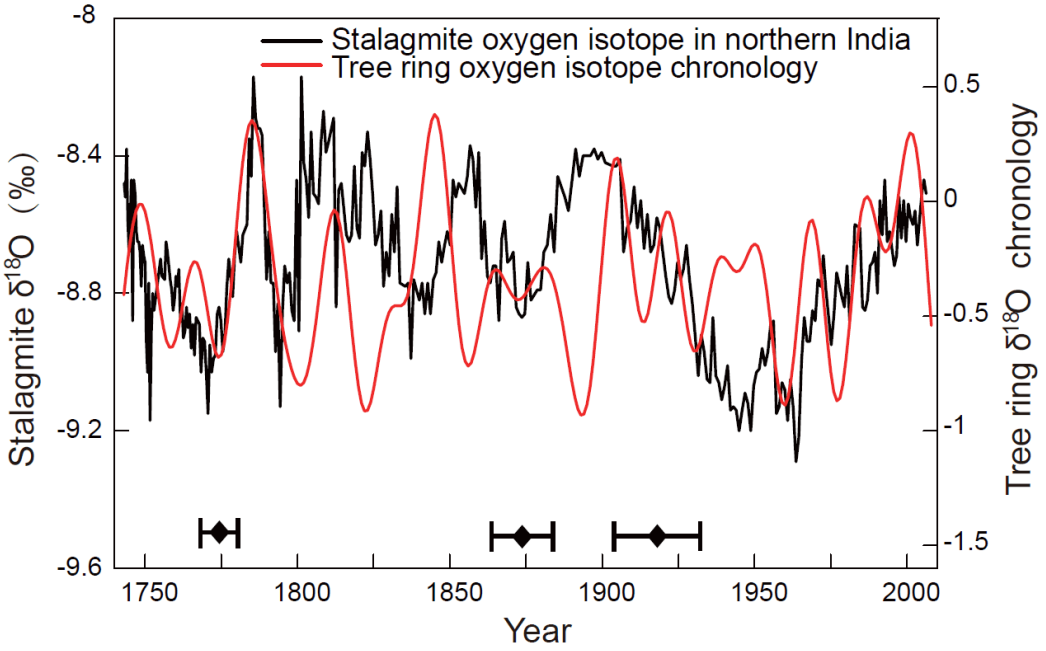

Figure 11. Comparison between multi-decadal regional tree ring $\delta^{18}O$ variations (red line) with stalagmite $\delta^{18}O$ changes (black line) in northern India. Rhombus with error indicates the ^{230}Th dates with uncertainty in stalagmite $\delta^{18}O$ chronology.